IEEE Access
Multidisciplinary : Rapid Review : Open Access Journal

Received April 20, 2022, accepted May 5, 2022, date of publication May 10, 2022, date of current version May 13, 2022.

Digital Object Identifier 10.1109/ACCESS.2022.3174100

Machine Learning-Based Estimation of Output Current Ripple in PFC-IBC Used in Battery Charger of Electrical Vehicles: A Comparison of LR, RF and ANN Techniques

FULYA ASLAY[1] AND NAIM SULEYMAN TING[2]
[1]Department of Computer Engineering, Erzincan Binali Yıldırım University, 24100 Erzincan, Turkey
[2]Department of Electrical Electronics Engineering, Erzincan Binali Yıldırım University, 24100 Erzincan, Turkey

Corresponding author: Naim Suleyman Ting (nsuleyman@erzincan.edu.tr)

ABSTRACT In this study, an artificial neural network (ANN) model is developed for the purpose of estimating the output current ripple of a power factor correction (PFC) AC/DC interleaved boost converter (IBC) used in battery charger of electrical vehicles (EVs) based on the inductance current ripple, switching frequency and load changes. Besides, the improved ANN model is compared with some different machine learning (ML) techniques like linear regression (LR), random forest (RF). The PFC-IBC is simulated with the PSIM simulation program to estimate the output current ripple. As a result, 336 output current ripple values are obtained based on inductance current ripple, different switching frequency and load changes. Then, the value of output current ripple is estimated by training the input parameters with LR, RF and ANN machine learning techniques (MLTs) for controlling the current harmonics drawn from the grid and for reliable charging of batteries. It is seen that the estimation value obtained with MLTs is quite compatible with the actual value obtained with the simulation. In addition, in the study carried out with the simulation, it takes a period of several days to obtain the estimation results; whereas, the operation of estimation with MLTs can be completed in a short period such as a few minutes. This clearly reveals the advantage of the MLTs. Therefore, this value is estimated through the MLTs with a high accuracy before the design of the charging device in order to maintain at a secure level the output current ripple posing considerable importance in electrical vehicle battery charge. Also, in this estimation process, LR, RF and developed ANN techniques are examined and compared separately in the WEKA program and it is observed that the developed ANN model proposes better results than other techniques.

INDEX TERMS Machine learning, artificial neural network, electrical vehicle, battery charging, power factor correction.

I. INTRODUCTION

Electrical vehicles (EVs) have an older history compared to the internal combustion engine vehicles, which are commonly used today. These vehicles are not able to show developments in those dates and are not intensively studied due to their long charging durations and low performance [1]. However, interest in EVs has increased again since fossil fuels have been gradually becoming exhausted recently when alternative energy resources are popular and the legal regulations have been enacted for decreasing the harmful gases emitted by the internal combustion engines to the atmosphere and environmental pollution.

The technology of electrical vehicle (EV) has been developing in three different ways as all-EVs, hybrid EVs, and fuel cell-EVs. The common point of these three technological advancements is the batteries used in the vehicle system and providing the chemical storage of the electrical energy. Aside from having high power and energy density for the batteries used, it is demanded for electrical vehicles to have fast charging ability and long life span [2], [3]. The battery system is an important factor among electrical vehicles. The distance of electrical vehicles is directly related to their battery capacities. Therefore, the need for batteries with higher

The associate editor coordinating the review of this manuscript and approving it for publication was Bilal Alatas.

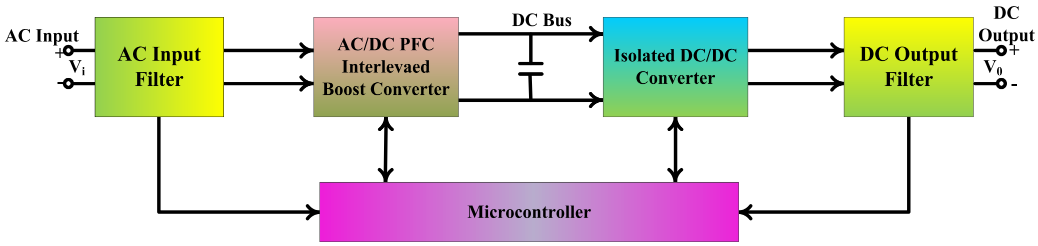

FIGURE 1. The inner structure of a typical switched charger.

energy capacity is gradually increasing. These advancements bring together the development of the chargers suitable for the needed infrastructure. Today, the charging devices commonly used on electrical vehicles are the ferro-resonant chargers, thyristor chargers, and switched chargers. The selection of the suitable charging device technology depends on the battery requirements and application needs. Ferro-resonant and thyristor chargers are durable and reliable and can endure for years. However, the switched chargers are better when compared to the ferro-resonant and thyristor chargers due to their characteristics such as being highly efficient, light-weight, low volume, quiet, and having the ability to respond fast to the changes [3]. Switched battery charger or in other words, the battery charge module, is an AC-DC/DC-DC converter implemented with a fully controlled semiconductor power switches. The response duration of these devices are very short since in these converters which are able to be operated at the considerably high frequencies since the turning on and off of the MOSFET and IGBTs are able to be controlled [4]–[6].

Figure 1 shows the structure of a typical switched charger. There is an AC filter in the input of switched charger. DC bus voltage is obtained through the interleaved boost converter (IBC) at the output of the rectifier by rectifying the AC filter output with the bridge diodes. The DC bus voltage is transferred to the output by regulating with an isolated DC-DC converter. The battery is charged by adjusting and filtering DC voltage obtained in the output. The harmonic components are generated at every stage of this process.

It is required to maintain the output current ripple of chargers at a certain level in order to guarantee the secure charging of electrical vehicle battery and their long life span. Having high output current ripples of battery chargers leads to the overheating of batteries and them having a shortened life span. In fact, since the battery management system would cut off the charge in the event of overheating, the battery of EV would not be completely charged with full capacity. Thus, the way the vehicle will make would restrict the distance, as well. For these reasons, it is quite important to estimate accurately the value of output current ripple, obtained in the DC-DC converter output, before the design in the design and control of the battery chargers [7]. At this point, machine learning (ML) techniques can be used. This is because ML techniques can offer much more practical, fast and accurate solutions in difficult mathematical calculations or applications that are difficult to test and measure. There are many ML techniques like linear regression (RL), random forest (RF), artificial neural network (ANN) etc. in the literature for estimation purpose [8]–[10]. The ANN technique is one of the mostly used techniques and it is a technique with a high accuracy rate [11]–[13].

TABLE 1. List of abbreviations.

ABBREVIATION	DESCRIPTION
EV	Electrical Vehicle
IBC	Interleaved Boost Converter
PFC	Power Factor Correction
ML	Machine Learning
MLT	Machine Learning Techniques
LR	Linear Regression
RF	Random Forest
ANN	Artificial Neural Network
D	Duty Cycle
THD	Total Harmonic Distortion
MLP	Multi-Layer Perceptron
MSE	Mean Square Error
R^2	Correlation Coefficient
MAE	Mean Absolute Error
RMSE	Root Mean Square Error
MAPE	Mean Absolute Percentage Error
MASE	Mean Absolute Scaled Error

In the study [14], a fault diagnosis is made for an inverter by giving input fault information with ML techniques. In [15], the useful life of the IGBT power element has been studied. In the study [16], a modeling is done for a DC-DC converter using the RF technique and so, it is seen that the machine learning based models is able to provide very close responses to the simulation results. In the study [17], the solar panel powers to be connected to the grid are estimated using the decision tree algorithm. In the study [18], the performance of a soft switched single phase inverter is examined as a result of its ANN control. In the study [19], the performance of operation of an asymmetric half bridge DC–DC converter with ANN is investigated.

In this study, an ANN model is suggested for the purpose of estimating the output current ripple of a power factor correction (PFC) - IBC used in the battery charger of electrical vehicles, based on inductance current ripple, frequency and load changes. The PFC-IBC used in the charger is simulated in PSIM program. 336 data are obtained as a result of the simulation and 315 of them are used for training the network and 21 of them are used in the suggested ANN model for testing. The estimation results obtained through ANN are considerably close to the results obtained with simulation, and it is possible to reach the estimation results in a much shorter time. In this way, a great ease is provided for electrical vehicle battery device designers with the developed ANN model, and it is possible to provide an optimum charger design by saving time. Besides, all the procedures to verify the presented ANN model are repeated with LR and RF ML techniques in the WEKA programme, and the results of these techniques are obtained. The results obtained with these three ML techniques are compared with a table and the superiority of the presented ANN model is demonstrated.

II. POWER FACTOR CORRECTION INTERLEAVED AC/DC BOOST CONVERTER

The spread of charges including non-linear units such as inverter and battery chargers leads to a significant increase in the voltage deformations and current harmonic distortion on electricity distribution systems. These harmonics may cause many problems including extreme neutral currents and the overheating of transformers on the power system. In order to decrease these harmonics negatively affecting the grid and increase the power factor, AC/DC power converters are used in battery charging. These converters are usually preferred as buck, boost and buck-boost converters. In the study proposed in [20], a buck converter is used has also been mitigated by applying the larger duty-cycle percentage variable width PWM signals. In the study proposed in [21], the PFC controller regulates the battery voltage and controls the supply current of the converter to achieve unity power factor. In addition to these, boost converters are also widely used [22], [23]. Passive and active methods are used depending on the charge and application type for the power factor correction. Both methods have advantages and disadvantages. In passive methods, coils and condensers are connected to the rectifier input or output in order to correct the input current. This system having a simple structure is quite awkward due to the use of the grid frequency inductances and capacitances. In addition, the power factor in this system is quite low and there are huge ripples in the non-controlled output voltage [24]. In the active method intensively studied in recent years, it is tried to converge the current towards the sinus form and regulate the output voltage by connecting a type of boost DC-DC converter on the rectifier output in general. A separate circuit can also be used for the regulation of the output voltage [25].

In the recent years, IBC obtained through the parallelization of classic boost converters is preferred in high power applications. The voltage applied to the input in the classical boost converter circuit shown in Figure 2 is rectified through the diode bridge and the rectified voltage is transferred to the output by boosting. These converters used commonly especially in PFC applications are usually operated in continuous current mode.

The converter shown in Figure 3 is an IBC circuit. Particularly in high power applications, the parallel operation (interleaved structure) of lower power boost converters is suggested for the same power instead of a single booster converter in order to decrease the high current stress on the circuit elements and use smaller circuit elements [26].

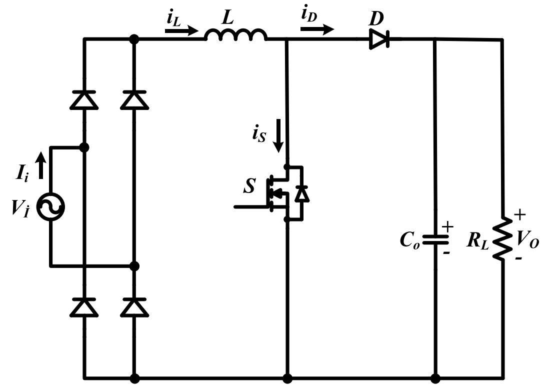

FIGURE 2. The classical boost converter circuit.

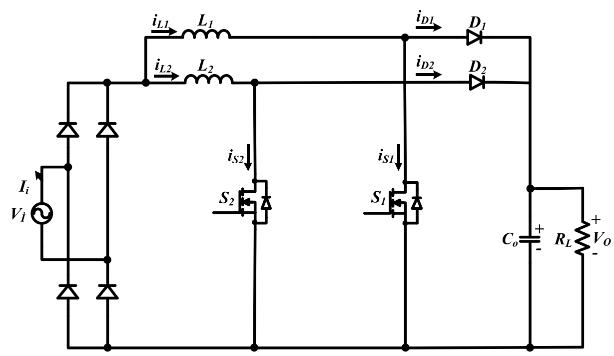

FIGURE 3. The interleaved boost converter circuit.

In operated studies using IBC, better performance can be provided compared to the classical boost converters. This is because IBC has many advantages such as lower input current and output voltage ripple, fast transmission response, lower input filter dimensions and low current stress on semiconductor devices when compared to the classical boost converters for the same power conditions [27]–[29].

Figure 4 shows wave forms of input inductance currents based on having higher or smaller than 50% of duty cycle (D). One of the most significant reasons for using IBC in this study is because the input current ripple is lower when compared to the classical boost converter. Thus, the current harmonics drawn from the grid and the total harmonic distortion (THD) in the battery charge are minimized. As seen from Figure 4, the average of L_1 and L_2 inductance currents provides the input current ripple. The equations between the input and

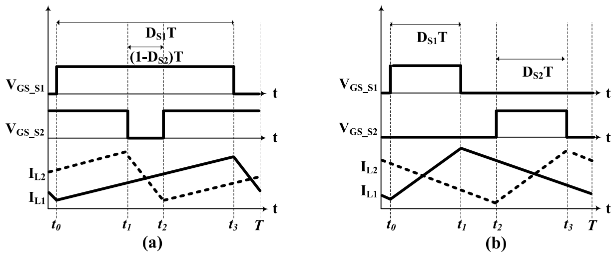

FIGURE 4. Control signals of the switches and the waveforms of boost inductor currents in (a) D > 50% mode, (b) D < 50% mode.

output voltages for each of the switches in the converter can be provided as follows for the turning-on and off condition of a switch;

$$\sum_{S_1=on} \Delta i_{L1} = \frac{V_i \cdot (D_{S1}T)}{L_1} \tag{1}$$

$$\sum_{S_1=off} \Delta i_{L1} = \frac{(V_o - V_i) \cdot [1 - (D_{S1}T)]}{L_1} \tag{2}$$

So, the input and output voltage ratio can be derived from eq. (1) and (2) as:

$$\frac{V_o}{V_i} = \frac{1}{1 - (D_{S1})} \tag{3}$$

III. MACHINE LEARNING (ML) TECHNIQUES-BASED ESTIMATION

Machine learning is the ability of machines to extract data without being explicitly programmed. It is an artificial intelligence application or subset that enables learning. In artificial intelligence, making a goal-oriented prediction or decision making is done by machine learning methods. There are extensive machine learning methods in the literature, some of which are; support vector machines are logistic regression, linear regression, simple bayes, k nearest neighbor, random forest, ANN and decision tree.

In this study, LR, RF and ANN techniques from machine learning techniques are used. The performance of the ANN model developed for estimation of output current ripple in PFC-IBC used in battery charger of electrical vehicles is compared with the LR and RF techniques.

A. LINEAR REGRESSION (LR)

Linear regression is a well-known and frequently used algorithm in statistics and machine learning. Linear regression models a target predictive value based on independent variables. It is mostly used to find the relationship between variables and prediction [9]. Different regression models differ in the relationship between dependent and independent variables and the number of independent variables used [30].

Linear regression's general equation is

$$y = c + mx \tag{4}$$

c is the y-intercepts and m is the slope.

The best fit line is

$$y = mx \tag{5}$$

In statistics, this equation is being represented generally as

$$y = \beta_0 + \beta_1 x_1 \tag{6}$$

If (x_1, x_2, …, x_n) are the n number of predictors then the equation is

$$y = \beta_0 + \beta_1 x_1 + \ldots\ldots.. + \beta_n x_n \tag{7}$$

B. RANDOM FOREST (RF)

Random Forest, like other classification methods, is used as a supervised machine learning method to apply classification and regression. As the name suggests, it creates a random forest. The created forest is usually a collection of decision trees trained by the "bagging" method. The purpose of the bagging method is that a combination of learning models increases the overall result [30].

RF technique does not experience outlier, excessive noise and overfitting problems. It also gives more accurate results than Decision trees and AdaBoost method, and it works faster than bagging and boosting methods [31]. The RF technique is a preferred method because of its features such as being able to perform multiple classifications and regressions, being able to be used for large-sized data sets, working quickly in training and testing stages, weighting for different classes and providing visualization [32].

C. ARTIFICAL NEURAL NETWORK (ANN)

Artificial neural network (ANN) is an information processing system inspired by biological neural networks and containing some performance features similar to biological neural networks [33]. ANNs, which simply imitate the way the human brain works, can learn from data, generalize, work with an unlimited number of variables, etc. It has many important features.is one of the powerful and general purpose data mining methods and can be applied in estimation, classification, and grouping problems.

The smallest unit of ANN is called artificial neuron or processing element. The simplest artificial neuron consists of 5 main components: inputs, weights, coupling function, activation function and output. Inputs (x_1, x_2…x_n) are information entering the cell from other cells or external environments. These are determined by the examples the network is asked to learn. Weights (w_1, w_2….w_n) are values that express the effect of another processing element in the input set or a previous layer on this processing element. Each input is aggregated through the sum function, multiplied by the weight that connects that input to the processing element. The sum function is as follows.

$$net = \sum_{i=1}^{n} w_i x_i + b \tag{8}$$

The output of the processing element is calculated by passing the value obtained as a result of the sum function

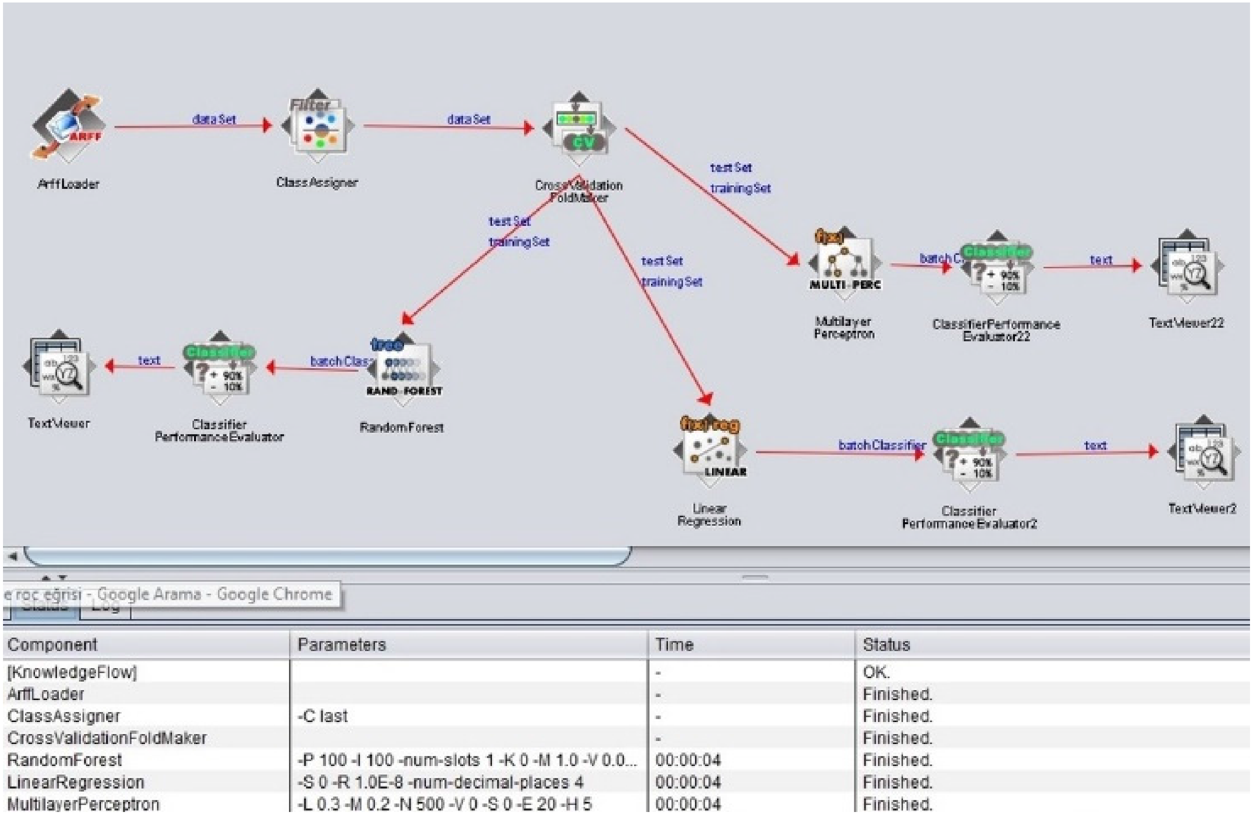

FIGURE 5. The knowledge flow of the used techniques in WEKA.

through a linear or nonlinear differentiable transfer function.

$$y = f\,(net) = f\left(\sum_{i=1}^{n} w_i x_i + b\right) \tag{9}$$

A multi-layer perceptron (MLP) artificial neural network is used in this study. MLP is a forward-looking neural network with one or more layers between the input and output layers. Feedforward means that data flows in a (forward) direction from the input to the output layer. This type of network is trained with back propagation learning algorithm. MLPs are widely used for pattern classification, recognition, prediction and approximation. MLP can solve non-linearly separated problems. A MLP is a forward-looking neural network that contains one or more layers between the input and output layers. Feedforward means that data flows in a (forward) direction from the input to the output layer. This type of network is trained with back propagation learning algorithm. MLPs are widely used for pattern classification, recognition, prediction and approximation. MLP can solve non-linearly separated problems.

Multilayer neural networks are used in solving complex problems, especially in predictions. Because in these networks, a series of operations in the structure of the hidden layer have the ability to automatically turn into a non-linear structure [34].

In this study these three supervised machine learning techniques, namely LR, RF and ANN are built using the WEKA Explorer module. These techniques are classification models. In the Classify tab of the WEKA Explorer 10-fold cross-validation testing and a batch size of 100 is used for all the optimization trials. The knowledge flow of the used techniques are displayed in Figure 5.

The results of LR, RF and developed ANN model in this study are given based on mean square error (MSE), root mean square error (RMSE), correlation coefficient (R^2), mean absolute error (MAE) metrics, mean absolute percentage error (MAPE) and mean absolute scaled error (MASE). MSE is the value obtained by adding the difference of the data values observed and estimated in the series, and dividing it into the total data number. It is the parameter quadratically indicating the error between the desired value and the output generated by the prediction model. This value being close to zero indicated that the estimated value converged strongly to the line. RMSE is a quadratic metric that measures the magnitude of error of a machine learning model, which is often used to find the distance between the predictor's predicted values and the true values. The RMSE is the standard deviation of the estimation errors. A zero RMSE value means that the model made no errors.

R^2 indicates how much of the change in the dependent variable can be explained by the independent variable.

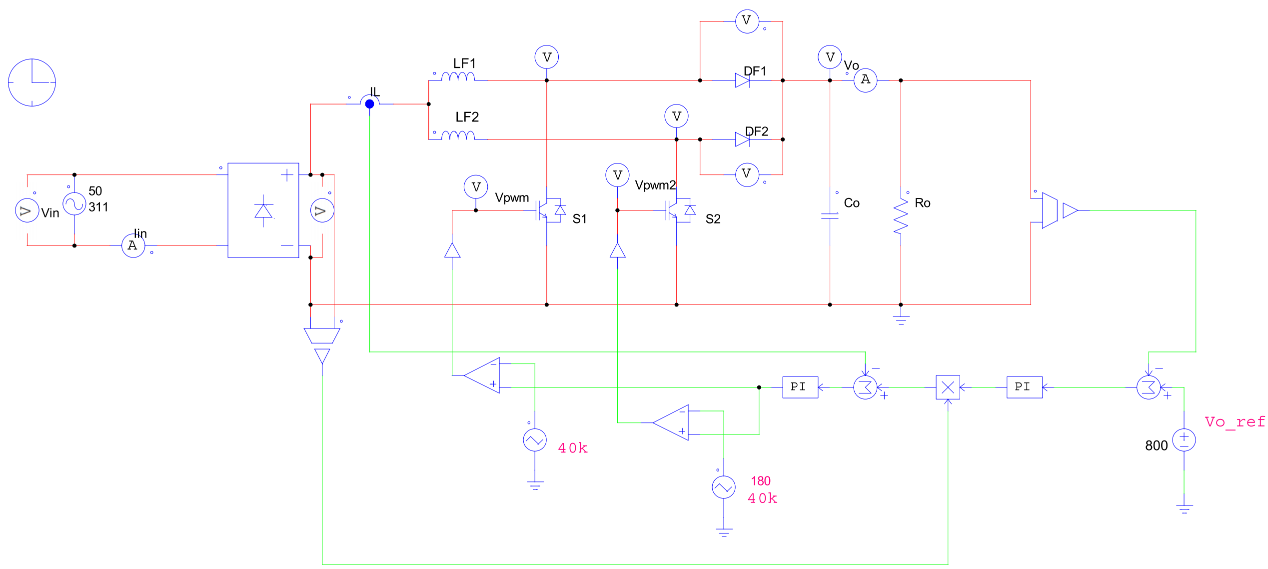

FIGURE 6. Simulation circuit schema and control block of the PFC-IBC converter.

The determination coefficient range equal to the square of the correlation coefficient is indicated with the equation $0 \leq R^2 \leq 1$. This value being close to 1 indicates that a great part of the variance in the dependent variable explains the independent variable in the model.

MAE represents the absolute mean error and is used to measure errors in the forecasting model. It shows how close the estimated value is to the actual value. MAPE is the demonstration of the average absolute values of errors as the percentage of actual values. The estimation models having a MAPE value under 10% are classified as having ''high accuracy'' level; whereas the models having a value between 10% and 20% are classified as accurate estimations. MASE is the mean absolute error of the forecast values, divided by the mean absolute error of the in-sample one-step naive forecast. It is a measure of the accuracy of predictions. The mean absolute scale error has favorable properties compared to other methods used to calculate forecast errors, such as root mean square deviation, and is therefore recommended for determining the comparative accuracy of forecasts [35].

The metrics used in the assessment of estimation results in this study are provided in the following equations, respectively. In the equations, O refers to the observed parameter and P refers to the predicted parameter.

$$MSE = \frac{1}{n}\sum_{i=1}^{n}(O_i - P_i)^2 \tag{10}$$

$$RMSE = \sqrt{\frac{1}{n}\sum_{i=1}^{n}(O_i - P_i)^2} \tag{11}$$

$$R^2 = \frac{\sum_{i=1}^{n}(O_i - O_{ave})(P_i - P_{ave})}{\sqrt{\sum_{i=1}^{n}(O_i - O_{ave})\sum_{i=1}^{n}(P_i - P_{ave})}} \tag{12}$$

$$MAE = \frac{1}{n}\sum_{i=1}^{n}|O_i - P_i| \tag{13}$$

$$MAPE = \frac{1}{n}\sum_{i=1}^{n}\left|\frac{O_i - P_i}{O_i}\right| \times 100 \tag{14}$$

$$MASE = \frac{\frac{1}{n}\sum_{i=1}^{n}|O_i - P_i|}{\frac{1}{n-1}\sum_{i=2}^{n}|P_i - P_{i-1}|} \tag{15}$$

IV. RESULTS AND DISCUSSION

Figure 6 shows the simulation circuit schema of the PFC-IBC converter which is used in the study and its data of which are obtained from PSIM 9.1.1 program. The reference measurements taken from the input and output by using PI controllers are included in control block so that the control signals of the semiconductor power switches in the IBC are obtained for PFC purpose. The data obtained from the simulation study are separated as training and testing data and used in the developed ANN model. The PFC operation of the converter is also experimentally verified by setup an experimental circuit prototype of the converter. The experimental circuit prototype photograph of the converter is given in Figure 7.

Figure 8 shows the simulation and experimental results of PFC-IBC. As shown in Figure, the results obtained from the simulation and the results obtained from the experimental study are compatible with each other. The input current and voltage waveforms are approximately in phase and the power factor is measured as 0.998. Therefore, the PFC process is successful.

By several machine learning techniques in this study, the value of output current ripple (ΔI_o) is estimated as output parameter when the input parameters are switching frequency (f_p), load resistance (R_L) and boost inductance current ripple (ΔI_L). Table 2 shows all the input and output parameter values in the converter used in the simulation study consisting of the used techniques. In here, the switching frequency (f_p) is

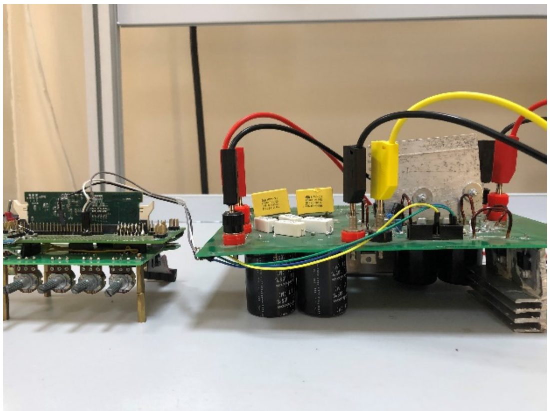

FIGURE 7. The experimental prototype of PFC-IBC converter.

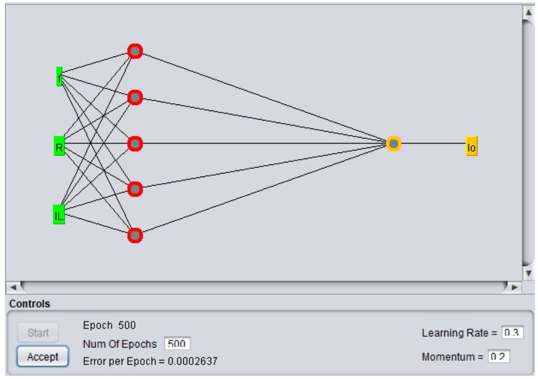

FIGURE 9. ANN model structure for output current ripple.

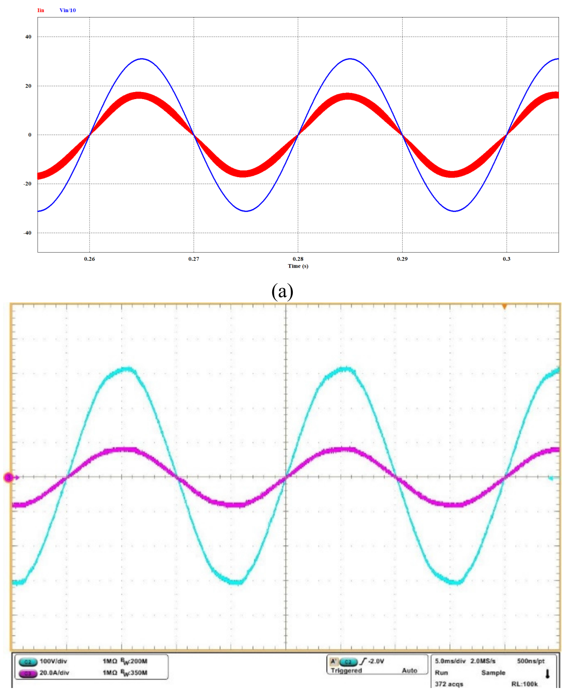

(a)

(b)

FIGURE 8. The input voltage and current waveforms obtained from a) simulation results and b) experimental results of the PFC-IBC converter.

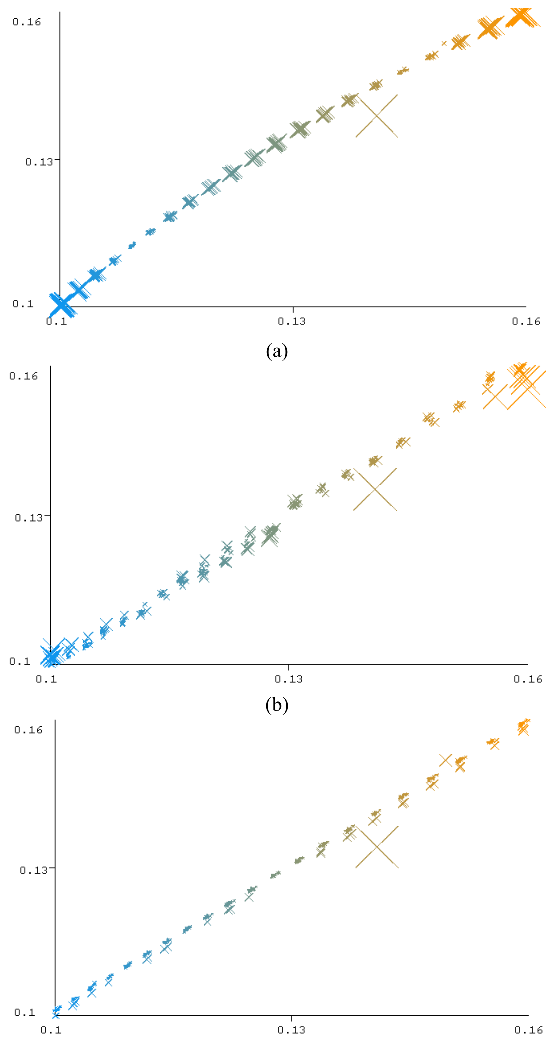

(a)

(b)

(c)

FIGURE 10. Overlap graphics of real and estimation results of machine learning techniques used for output current ripple estimation with a) LR b) RF c) ANN.

TABLE 2. The parameters of circuit.

Parameter	Symbol	Value
Input Voltage	V_i	220 V_{AC}
Output Voltage	V_O	800 V_{DC}
Output Capacitor	C_o	470 µF
Boost Inductors	L_1, L_2	750 µH
Switching Frequency	f_p	10-40 kHz (Variable in 2 kHz intervals)
Load Resistance	R_L	160-200 Ω (Variable in 2 Ω intervals)

increased in twos between 10-40 kHz and the load resistance (R_L) is increased in twos between 160-200 Ω in the data set in this study. Thus, 336 data is obtained from simulation operation in total.

Figure 9 shows the structure of the ANN model generated for the estimation of output current ripple. In the optimum model generated for the study after the made many tests, there are a three-neural input layer, a five-neural secret layer and a single neural output layer as seen from figure.

Fig. 10 shows the overlap graphics of real and estimation results of machine learning techniques used for output current ripple estimation with LR, RF and ANN techniques. As shown in Figure, in all three ML techniques, the actual measurement results and the estimation results overlap, and thus, it is observed that the estimation results are very close to the real results.

In this study three supervised machine learning techniques, namely LR, RF and ANN are built using the WEKA Explorer module. These techniques are classification models. For the estimation of the output current ripple (ΔI_o), the predictive power of the models are evaluated with the performance criteria of R^2, MSE, RMSE, MAE, MASE and MAPE and the results are listed in Table 3. According to these results, R^2, MSE, RMSE, MAE, MASE and MAPE values of ANN model are calculated as 0.9995, 0.0006, 0.0245, 0.0002, 0.0714 and 0.2216, respectively. By considering these values, it seems that ANN model is more successful than the LR and RF models.

TABLE 3. The comparison of the machine learning techniques.

MODEL	R^2	MSE	RMSE	MAE	MASE	MAPE
LR	0.9957	0.0016	0.0398	0.0014	0.4912	0.9935
RF	0.9979	0.0008	0.0283	0.0012	0.4285	0.7630
ANN	0.9995	0.0006	0.0245	0.0002	0.0714	0.2216

V. CONCLUSION

In this study, an ANN model is developed for the purpose of estimating the output current ripple of a PFC AC/DC interleaved boost converter used in battery charger of electrical vehicles based on the inductance current ripple, switching frequency and load changes. Besides, the improved ANN model is compared with some different machine learning techniques like linear regression, random forest. The dataset used for estimation is obtained by simulating the converter in the PSIM 9.1.1 program. In this study, not only the power factor is corrected, but also the estimation of output current ripple is separately made through LR, RF MLTs and the ANN model developed for the secure charging of the battery. The MLTs estimation results are compared based on the R^2, MSE, RMSE, MAE, MASE and MAPE performance criteria. It is observed that the developed ANN model is more successful than the LR and RF techniques. In ANN model, R^2, MSE, RMSE, MAE, MASE and MAPE values are calculated as 0.9995, 0.0006, 0.0245, 0.0002, 0.0714 and 0.2216, respectively. Consequently, a highly accurate estimation is made with the developed ANN model. Due to this estimation is produced in a much shorter time than the simulation, the output current fluctuation can be predicted in order to ensure reliable charging and longer life of electric vehicle batteries, providing both time saving and convenience for charger designers.

REFERENCES

[1] J. K. Nor, "Art of charging electric vehicle batteries," in *Proc. WESCON*, San Francisco, CA, USA, Sep. 1993, pp. 521–525.

[2] A. Khaligh and Z. Li, "Battery, ultracapacitor, fuel cell, and hybrid energy storage systems for electric, hybrid electric, fuel cell, and plug-in hybrid electric vehicles: State of the art," *IEEE Trans. Veh. Technol.*, vol. 59, no. 6, pp. 2806–2814, Jul. 2010.

[3] I. A. Khan, "Battery chargers for electric and hybrid vehicles," in *Proc. IEEE Workshop Power Electron. Transp.*, Oct. 1994, pp. 103–112.

[4] B. J. Masserant and T. A. Stuart, "A maximum power transfer battery charger for electric vehicles," *IEEE Trans. Aerosp. Electron. Syst.*, vol. 33, no. 3, pp. 930–938, Jul. 1997.

[5] M. M. Morcos, N. G. Dillman, and C. R. Mersman, "Battery chargers for electric vehicles," *IEEE Power Eng. Rev.*, vol. 20, no. 11, pp. 8–11, Nov. 2000.

[6] C. E. S. Thomas, "Transportation options in a carbon-constrained world: Hybrids, plug-in hybrids, biofuels, fuel cell electric vehicles, and battery electric vehicles," *Int. J. Hydrogen Energy.*, vol. 34, pp. 9279–9296, Dec. 2009.

[7] V.-S. Nguyen, V.-L. Tran, W. Choi, and D.-W. Kim, "Analysis of the output ripple of the DC-DC boost charger for li-ion batteries," *J. Power Electron.*, vol. 14, no. 1, pp. 135–142, Jan. 2014.

[8] G. Shanmugasundar, M. Vanitha, R. Cep, V. Kumar, K. Kalita, and M. Ramachandran, "A comparative study of linear, random forest and adaboost regressions for modeling non-traditional machining," *Processes*, vol. 9, no. 11, p. 2015, 2021.

[9] K. K. Gupta, K. Kalita, R. K. Ghadai, M. Ramachandran, and X. Z. Gao, "Machine learning-based predictive modelling of biodiesel production—A comparative perspective," *Energies*, vol. 14, no. 4, p. 1122, 2021.

[10] O. Arikan, C. C. Uydur, and C. F. Kumru, "Prediction of dielectric parameters of an aged mv cable: A comparison of curve fitting, decision tree and artificial neural network methods," *Electr. Power Syst. Res.*, vol. 208, Jul. 2022, Art. no. 107892.

[11] A. Anzalchi and A. Sarwat, "Artificial neural network based duty cycle estimation for maximum power point tracking in photovoltaic systems," in *Proc. IEEE Int. Southeast Conf.*, Fort Lauderdale, FL, USA, Apr. 2015, pp. 1–5.

[12] M. T. Makhloufi, Y. Abdessemed, and M. S. Khireddine, "An efficient ANN-based MPPT optimal controller of a DC/DC boost converter for photovoltaic systems," *Automatika*, vol. 57, no. 1, pp. 109–119, Jan. 2016.

[13] J. N. Marie-Francoise, H. Gualous, and A. Berthon, "DC to DC converter with neural network control for on-board electrical energy management," in *Proc. 4th Int. Power Electron. Motion Control Conf.*, Xi'an, China, Aug. 2004, pp. 521–525.

[14] S. Khomfoi and L. M. Tolbert, "Fault diagnostic system for a multilevel inverter using a neural network," *IEEE Trans. Power Electron.*, vol. 22, no. 3, pp. 1062–1069, May 2007.

[15] A. Alghassi, S. Perinpanayagam, and M. Samie, "Stochastic RUL calculation enhanced with TDNN-based IGBT failure modeling," *IEEE Trans. Rel.*, vol. 65, no. 2, pp. 558–573, Jun. 2016.

[16] H. S. Krishnamoorthy and T. Narayanan Aayer, "Machine learning based modeling of power electronic converters," in *Proc. IEEE Energy Convers. Congr. Expo. (ECCE)*, Oct. 2019, pp. 666–672.

[17] J. Wang, P. Li, R. Ran, Y. Che, and Y. Zhou, "A short-term photovoltaic power prediction model based on the gradient boost decision tree," *Appl. Sci.*, vol. 8, no. 5, p. 689, Apr. 2018.

[18] A. P. N. Ismayil Kani, S. P. B. V. Manikandan, and A. P. K. Premkumar, "Performance of single phase soft switching inverter using artificial neural network," *Microprocessors Microsyst.*, to be published, doi: 10.1016/j.micpro.2021.104236.

[19] A. Gnanasaravanan and M. Rajaram, "Artificial neural network for monitoring the asymmetric half bridge DC–DC converter," *Int. J. Elect. Power Energy Syst.*, vol. 43, pp. 788–792, Dec. 2012.

[20] S. Das, K. M. Salim, and D. Chowdhury, "A novel variable width PWM switching based buck converter to control power factor correction phenomenon for an efficacious grid integrated electric vehicle battery charger," in *Proc. IEEE Region 10 Conf. (TENCON)*, Penang, Malaysia, Nov. 2017, pp. 262–267.

[21] S. Ketsingsoi and Y. Kumsuwan, "An off-line battery charger based on buck-boost power factor correction converter for plug-in electric vehicles," *Energy Proc.*, vol. 56, pp. 659–666, Jan. 2014.

[22] O. García, J. A. Cobos, R. Prieto, and J. Uceda, "Single phase power factor correction: A survey," *IEEE Trans. Power Electron.*, vol. 18, no. 3, pp. 749–755, May 2003.

[23] M. Fariborz, E. Wilson, and W. G. Dunford, "A high-performance single-phase bridgeless interleaved PFC converter for plug-in hybrid electric vehicle battery chargers," *IEEE Trans. Ind. Appl.*, vol. 47, no. 4, pp. 1833–1843, Jul./Aug. 2011.
[24] C. Qiao and K. M. Smedley, "A topology survey of single-stage power factor corrector with a boost type input-current-shaper," *IEEE Trans. Power Electron.*, vol. 16, no. 3, pp. 360–368, May 2001.
[25] O. Garcia, J. A. Cobos, R. Prieto, P. Alou, and J. Uceda, "Power factor correction: A survey," in *Proc. IEEE 32nd Annu. Power Electron. Spec. Conf.*, Vancouver, BC, Canada, Jun. 2001, pp. 8–13.
[26] N. S. Ting, Y. Sahin, and I. Aksoy, "Analysis, design, and implementation of a zero-voltage-transition interleaved boost converter," *J. Power Electron.*, vol. 17, no. 1, pp. 41–55, Jan. 2017.
[27] M. Esteki, B. Poorali, E. Adib, and H. Farzenahfard, "Interleaved buck converter with continuous input current, extremely low output current ripple, low switching losses, and improved step-down conversion ratio," *IEEE Trans. Ind. Electron.*, vol. 62, no. 8, pp. 4769–4776, Aug. 2015.
[28] M. Esteki, B. Poorali, E. Adib, and H. Farzanehfard, "High step-down interleaved buck converter with low voltage stress," *IET Power Electronics.*, vol. 8, no. 12, pp. 2352–2360, 2015.
[29] K. H. M. S. Chao Yang, "High step-up interleaved converter with soft-switching using a single auxiliary switch for a fuel cell system," *IET Power Electron.*, vol. 7, no. 11, pp. 2704–2716, Nov. 2014.
[30] A. Dey, "Machine learning algorithms: A review," *Int. J. Comput. Sci. Inf. Technol.*, vol. 7, no. 3, pp. 1174–1179, 2016.
[31] L. Breiman, "Random forests," *Mach. Learn.*, vol. 45, no. 1, pp. 5–32, 2001.
[32] A. Cutler, D. R. Cutler, and J. R. Stevens, "Random forests," *Mach. Learn.*, vol. 45, no. 1, pp. 157–176, 2011.
[33] L. Fausett, *Fundamentals of Neural Networks: Architectures, Algorithms and Applications*. Upper Saddle River, NJ, USA: Prentice-Hall, 1994.
[34] G. Zhang, B. E. Patuwo, and M. Y. Hu, "Forecasting with artificial neural networks: The state of the art," *Int. J. Forecasting*, vol. 14, pp. 35–62, 1998.
[35] R. J. Hyndman and A. B. Koehler, "Another look at measures of forecast accuracy," *Int. J. Forecasting*, vol. 22, no. 4, pp. 679–688, Oct. 2006.

FULYA ASLAY was born in Erzincan, Turkey, in 1983. She received the B.S. degree in computer engineering from Trakya University, Tekirdağ, Turkey, in 2005, and the M.S. and Ph.D. degrees in management information systems from Ataturk University, Erzurum, Turkey, in 2009 and 2013, respectively. She has been an Assistant Professor with the Department of Computer Engineering, Erzincan Binali Yıldırım University, since 2013. Her research interests include computer sciences, database and data structures, management information systems, artificial intelligence, computer learning, and pattern recognition. She has published over 40 journals and conference papers in these areas.

NAIM SULEYMAN TING was born in Erzurum, Turkey, in 1988. He received the B.S. degree from Erciyes University, Kayseri, Turkey, in 2010, and the M.S. and Ph.D. degrees in electrical engineering from Yildiz Technical University, İstanbul, Turkey, in 2013 and 2016, respectively. He has been an Associate Professor with the Department of Electrical Electronics Engineering, Erzincan Binali Yıldırım University. His research interests include soft switching, power factor correction, switching power supplies, high frequency power conversion, and active and passive snubber cells in power electronics. He has published over 50 journals and conference papers in these areas.